Exploring the Immunotherapeutic Potential of Oleocanthal against Murine Cutaneous Leishmaniasis#

OPEN ACCESS

Authors

Kalliopi Karampetsou[1,2], Olga S. Koutsoni[1], Fotis Badounas[3], Apostolis Angelis[2], Georgia Gogou[1,2], Leandros-Alexios Skaltsounis[2], Maria Halabalaki[2], Eleni Dotsika[1]

Affiliations

1 Laboratory of Cellular Immunology, Department of Microbiology, Hellenic Pasteur Institute, Athens, Greece
2 Division of Pharmacognosy and Natural Product Chemistry, Department of Pharmacy, National and Kapodistrian University of Athens, Athens, Greece
3 Molecular Genetics Laboratory, Department of Immunology, Transgenic Technology Laboratory, Hellenic Pasteur Institute, Athens, Greece

Key words

Olea europaea L. *(Oleaceae)*, cutaneous leishmaniasis, oleocanthal, *in vitro* and *in vivo* antileishmanial effect, immunomodulation

received	November 11, 2021
accepted after revision	March 27, 2022
published online	July 8, 2022

Bibliography

Planta Med 2022; 88: 783–793

DOI 10.1055/a-1843-9788

ISSN 0032-0943

Georg Thieme Verlag KG, Rüdigerstraße 14, 70469 Stuttgart, Germany

Correspondence

Dr. Eleni Dotsika
Department of Microbiology, Laboratory of Cellular Immunology, Hellenic Pasteur Institute
127 Vass. Sofias Av., 11521 Athens, Greece
Phone: + 30 21 06 47 88 28, Fax: + 30 21 06 47 88 28
e.dotsika@pasteur.gr

Correspondence

Associate Professor Maria Halabalaki
Department of Pharmacy, Division of Pharmacognosy and Natural Product Chemistry, National and Kapodistrian University of Athens
15771 Athens, Panepistimiopolis, Greece
Phone: + 30 21 07 27 47 81, Fax: + 30 21 07 27 45 94
mariahal@pharm.uoa.gr

ABSTRACT

Leishmaniasis is a major tropical disease with increasing global incidence. Due to limited therapeutic options with severe drawbacks, the discovery of alternative treatments based on natural bioactive compounds is important. In our previous studies we have pointed out the antileishmanial activities of olive tree-derived molecules. In this study, we aimed to investigate the *in vitro* and *in vivo* antileishmanial as well as the *in vivo* immunomodulatory effects of oleocanthal, a molecule that has recently gained increasing scientific attention. Pure oleocanthal was isolated from extra virgin olive oil through extraction and chromatography techniques. The *in vitro* antileishmanial effects of oleocanthal were examined with a resazurin-based assay, while its *in vivo* efficacy was evaluated in *Leishmania major*-infected BALB/c mice by determining footpad induration, parasite load in popliteal lymph nodes, histopathological outcome, antibody production, cytokine profile of stimulated splenocytes and immune gene expression, at three weeks after the termination of treatment. Oleocanthal demonstrated *in vitro* antileishmanial effect against both *L. major* promastigotes and intracellular amastigotes. This effect was further documented *in vivo* as demonstrated by the suppressed footpad thickness, the decreased parasite load and the inflammatory cell influx at the infection site. Oleocanthal treatment led to the dominance of a Th1-type immunity linked with resistance against the disease. This study establishes strong scientific evidence for olive tree-derived natural products as possible antileishmanial agents and provides an adding value to the scientific research of oleocanthal.

Dedicated to Professor Dr. A. Douglas Kinghorn on the occasion of his 75th birthday.

ABBREVIATIONS

b. w.	body weight
$CDCl_3$	deuterated chloroform
CL	cutaneous leishmaniasis
CPC	countercurrent partition chromatography
CPE	centrifugal partition extraction
DCM	dichloromethane
EVOO	extra virgin olive oil
HePC	hexadecylphosphocholine (miltefosine)
HRP	horseradish peroxidase
i. p.	intraperitoneally
LDA	limiting dilution assay
LN	lymph node
m/z	mass-to-charge ratio
NSAID	nonsteroidal anti-inflammatory drug
OD	optical density
OLEO	oleocanthal
s. c.	subcutaneously
SDS	sodium dodecyl sulfate
SLA	soluble *Leishmania* antigen
TPF	total phenolic fraction
UPLC	ultra-performance liquid chromatography
VOO	virgin olive oil

Introduction

CL is the most common clinical form of a widespread parasitic disease, with increasing incidence, caused by protozoan parasites of the *Leishmania* genus [1]. Prevention through vaccination is not available since an effective human vaccine does not yet exist and the main interventions consist of chemotherapeutic treatment. The available drug arsenal is limited and exhibits drawbacks, such as toxicity, poor efficacy, high cost, and parasite resistance [2]. Thus, the development of new treatment alternatives is an essential requirement that meets the WHO's response plan against leishmaniasis [3]. Over recent years, the search for naturally occurring compounds with pharmacological properties has been increased. Plant-derived products have been studied for treating various diseases, including leishmaniasis [4].

Products from the olive tree (*Olea europaea* L., *Oleaceae*), the most characteristic tree in Mediterranean countries, have gained scientific interest, since the overall health beneficial action of VOO through the Mediterranean diet is well established [5]. Several studies have assigned the beneficial biological properties of VOO, especially of EVOO, to its phenolic composition [6, 7]. Among the phenolic compounds of EVOO, OLEO, firstly documented in the 1990s, has attracted significant scientific attention. OLEO is homologous with the NSAID ibuprofen for both perceptual and anti-inflammatory features [8] and it has been reported to exhibit various modes of action in reducing the occurrence of inflammatory related diseases, such as neurodegenerative diseases and cancer [9]. Moreover, it has been associated with *in vitro* antimicrobial properties [8]. Our previous studies with an OLEO-enriched crude extract (TPF) and other pure natural agents, all derived from olive products, revealed their strong antileishmanial and immunomodulatory properties in *in vitro* and *in vivo* systems [10–12]. Additionally, various other studies demonstrated medicinal products of the olive tree that possess antileishmanial properties [13, 14], enhancing the position of the olive tree as a promising source for antileishmanial compounds.

In this study, we investigated, for the first time, the potential of pure OLEO to be used as an antileishmanial agent. We evaluated its *in vitro* antileishmanial properties against *Leishmania major* promastigotes and amastigotes as well as its *in vivo* efficacy in a murine experimental model of CL. We further revealed the immunomodulatory properties of OLEO and its ability to concomitantly eliminate *Leishmania* parasites and modify the host's immunity towards a protective immune response in a murine experimental model of CL.

Results

The antileishmanial activity of OLEO on *L. major* promastigotes and amastigotes was assessed by determining the IC_{50} (µg/mL) values using a resazurin-based cell viability assay. OLEO inhibited the growth of promastigotes (▶ **Fig. 1 a**) and amastigotes (▶ **Fig. 1 b**), presenting IC_{50} values of 18.7 and 87 µg/mL, respectively. The standard reference drug HePC was used at 6.4 µg/mL for promastigotes and 3.2 µg/mL for amastigotes, as was previously determined [11].

To evaluate the therapeutic potential of OLEO on the development of experimental CL, genetically susceptible BALB/c mice were firstly infected s. c. with stationary phase *L. major* promastigotes. The applied dose of OLEO (5 mg/kg b. w.) and the i. p. route of its administration were chosen according to relevant *in vivo* studies [15–18]. Clinical evaluation of toxicity was performed prior to the first administration and at weekly intervals during the administration period. To this end, we assessed feeding and drinking behavior, abnormal behavior in "handling", fur condition, posture, activity level, abnormal movements, gait abnormalities, and body weight and there was no clinical evidence of OLEO-caused toxicity.

In order to record the inflammation progression at the injection site, the footpad induration was monitored in all experimental animals once per week. The development of footpad lesions was monitored for up to 7 weeks postinfection (▶ **Fig. 2**). The administration of OLEO promoted a significant and constant reduction of footpad thickness, reaching 45 % compared to the control group of untreated mice, at 7 weeks postinfection (▶ **Fig. 2**). It is noteworthy that HePC exhibited equal suppression and lesion reduction compared to OLEO.

The parasite burden was evaluated in draining popliteal LNs by an LDA [19] 3 weeks after the termination of treatment. As depicted in ▶ **Fig. 3**, treatment with OLEO caused a significant fall (~ 1.6-fold) in parasite levels compared to untreated mice. HePC reduced the parasite load even more efficiently compared to OLEO (88 007 ± 27 243 vs. 124 523 ± 27 067, $p = 0.047$). Moreover, the weights of draining LNs in OLEO-treated mice were significantly decreased compared to untreated mice 3 weeks after the termination of treatment ($p = 0.024$) (▶ **Fig. 4**).

At the same time point, the infected paws were processed for histochemistry and immunohistochemistry analysis. The histopathological analysis revealed a pleomorphic inflammatory infil-

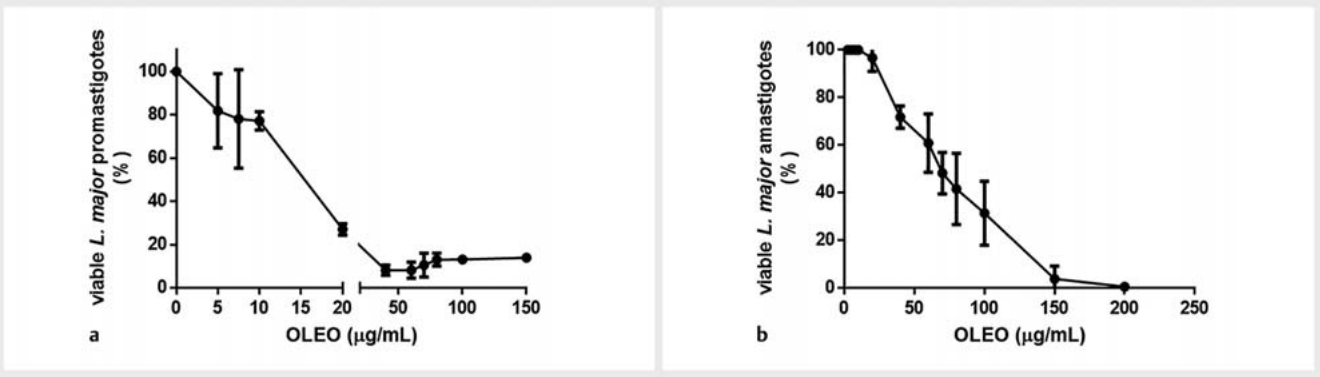

▶ **Fig. 1** Cell viability of *L. major* promastigotes and amastigotes exposed to OLEO. The antileishmanial effect of OLEO was tested on *L. major* promastigotes (**a**) and amastigotes (**b**) with a resazurin-based assay. Increasing concentrations of OLEO were added in tissue culture plates containing either promastigotes or *L. major*-infected J774A.1 macrophages and incubated at 26 °C for 60 h and at 37 °C under 5% CO_2 humidified air for 48 h, respectively. OD was determined with an absorbance microplate reader (excitation: 570 nm, reference filter: 630 nm). Data are presented as mean values ± SD of three independent experiments.

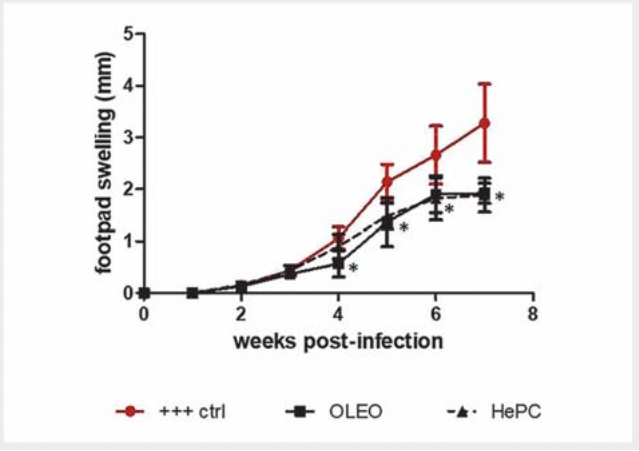

▶ **Fig. 2** Footpad induration throughout the treatment course. BALB/c mice were infected with 1×10^6 *L. major* promastigotes in the left hind footpad. Ten days later, mice were either treated with OLEO (n = 6) (5 mg/kg b.w., 3 ×/week for 16 total doses) or HePC (n = 6) (15 mg/kg b.w., 5 ×/week for 25 total doses) or left untreated (n = 6). Footpad thickness was monitored weekly. Data are presented as mean thickness ± SD. *Statistical difference compared to control (+++ctrl) group of untreated mice.

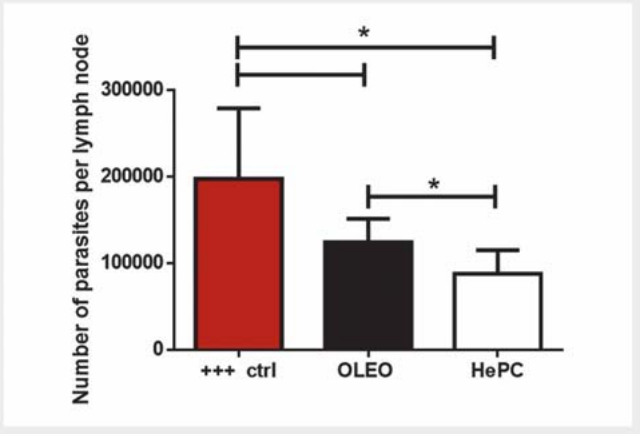

▶ **Fig. 3** Quantification of parasite burden in popliteal LNs. Parasite burden was estimated by LDA 3 weeks after the termination of treatment. Each bar represents the mean ± SD for each experimental group (n = 6/group). *Significant difference among groups.

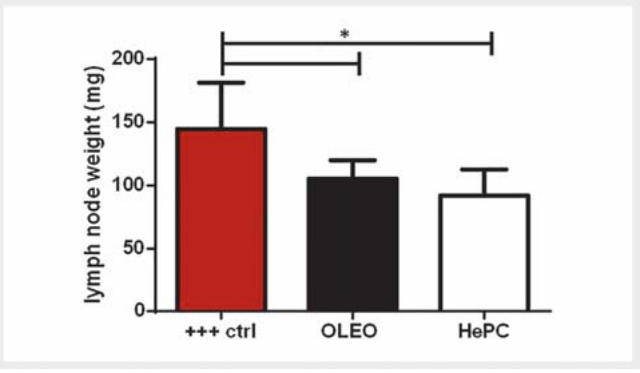

▶ **Fig. 4** Weights of draining popliteal LNs. Weights (n = 6/group) were measured 3 weeks after the termination of treatment. Results are expressed as mean values ± SD. *Significant difference among experimental groups.

trate with non-vacuolated and vacuolated parasite-containing macrophages with extensive necrotic areas surrounded by neutrophils in infected paws of OLEO-treated mice (▶ **Fig. 5a**), while untreated mice showed a diffuse infiltration of macrophages containing intact parasites (▶ **Fig. 5a**). In the OLEO-treated mice, it was also observed that focal aggregates of macrophages were intermixed with lymphocytes, as strongly suggested by the intense presence of CD3+ cell infiltrates (▶ **Fig. 5b**) and the presence of CD20+ cells (▶ **Fig. 5c**). Moreover, in OLEO-treated mice, we detected pronounced mast cell degranulation, predominantly located in the superficial dermis and near granuloma formations (▶ **Fig. 5d**).

Plasma was collected 3 weeks after treatment termination for the definition of *Leishmania*-specific isotype antibody response.

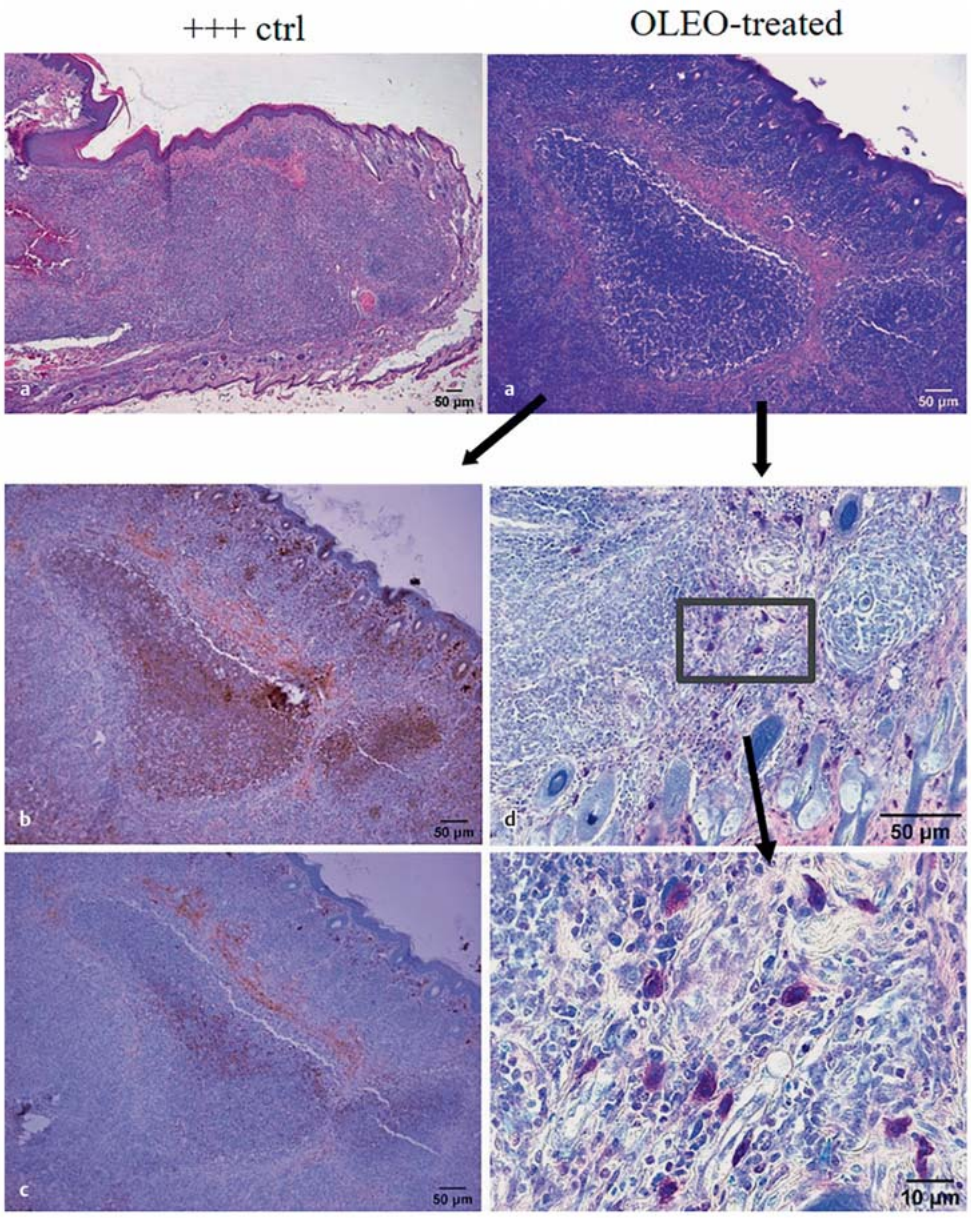

▶ **Fig. 5** Histopathological images of the infected paws from *L. major*-infected BALB/c mice 3 weeks after the termination of treatment with OLEO. BALB/c mice were infected with 1×10^6 promastigotes in the left hind footpad and either treated with OLEO (5 mg/kg b.w., 3 ×/week for 16 total doses) or HePC (15 mg/kg b.w., 5 ×/week for 25 total doses) or left untreated (+++ ctrl). **a** Representative H&E staining of lesion tissues from untreated and OLEO-treated mice. Multifocal necrotic granuloma formations with intense macrophage infiltrate in OLEO-treated mice are observed versus untreated mice (scale bar = 50 µm). **b** T-lymphocyte CD3+ infiltrate inside granuloma formation and (**c**) presence of CD20+ cells in OLEO-treated mice (scale bar = 50 µm). **d** Mast cell degranulation located in the superficial dermis in OLEO-treated mice, as indicated by Giemsa staining (scale bars = 50 and 10 µm).

Our results showed that levels of IgG1 in OLEO-treated mice were lower (1.6-fold) than untreated mice, while respective levels of IgG2a were higher (1.7-fold) (▶ **Fig. 6**).

Spleens were collected in order to estimate the type of induced cellular immunity. OLEO treatment significantly increased the proportion of $CD4^+$-$IL\text{-}12^+$-producing cells in the spleen compared to untreated mice ($p = 0.018$) 3 weeks posttreatment termination (▶ **Fig. 7**), while the proportions of $CD4^+$ T lymphocytes that expressed IFN-γ and IL-4 were equal.

For further clarification of the host's induced adaptive immunity, the expression of mRNAs encoding for *IL-12b* and *IL-4* cytokines and *Tbx21* and *GATA-3* transcription factors were analyzed as indicators of Th1- and Th2-type immune responses, respectively [20]. The *IL-12b*/*IL-4* and *Tbx21*/*GATA-3* gene expression ratios in OLEO-

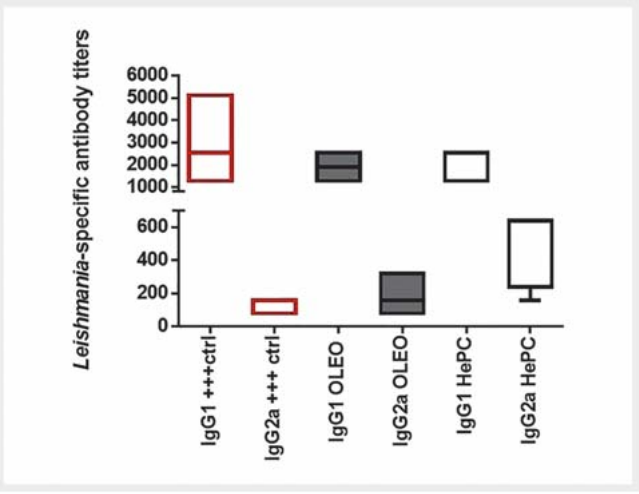

▶ **Fig. 6** Determination of *Leishmania*-specific antibody titers. Mean reciprocal antibody titers are represented as box-and-whisker plots showing the distribution of IgG1 and IgG2a in plasma of BALB/c mice 3 weeks after the termination of treatment. The horizontal line in the middle of each box indicates the median, whereas the top and bottom borders of the box mark the 90th and 10th percentile.

treated mice were 3- and 2.4-fold upregulated, respectively, compared to untreated mice ($p = 0.050$) (▶ **Fig. 8a, b**).

Discussion

Our research group developed an efficient separation process for the gram-scale isolation of pure OLEO [21, 22]. This procedure includes the initial CPE-based extraction of TPF from olive oil followed by chromatographic isolation of pure OLEO from TPF using an orthogonal combination of preparative CPC and HPLC analysis. The use of olive oil as part of the extraction biphasic system in combination with the state-of-the-art CPE/CPC technology makes the separation process green, efficient, and capable for pilot and industrial scale applications.

This study addresses, for the first time, according to our knowledge, the antileishmanial effect of purified OLEO from EVOO, as demonstrated by *in vitro* and *in vivo* experiments. OLEO exhibited an inhibitory effect *in vitro* against both the promastigote and intracellular amastigote forms of *L. major* parasites. These results are in accordance with our previous studies, indicating an OLEO-enriched phenolic fraction with a powerful inhibitory effect against *L. major* promastigotes and amastigotes [10]. Additionally, these data are in line with a recent study also demonstrating a powerful inhibitory effect of another natural product, 6-gingerol, against *L. major* promastigotes [23]. Although our previous studies with an OLEO-enriched TPF showed that promastigotes were more resistant compared to amastigotes [11], in the current study, the results suggest the contrary. As other researchers have suggested, the differences between the conditions of promastigotes and amastigotes cultures in pH and serum protein concentration can affect the availability of the tested drugs, therefore resulting in higher IC_{50} values for the amastigote forms of the parasite [24].

The therapeutic potential of OLEO was determined in genetically susceptible BALB/c mice infected with *L. major*, which constitutes a nonhealing model of CL, where the inadequate host's cells mediated immune response results in parasite persistence and chronic tissue ulceration [25]. Various doses and routes of administration have been used in different studies to assess the *in vivo* bioactivity of OLEO and negligible toxicity was reported [18, 26–28]. Our results indicated that OLEO-treated mice exhibited a remarkable reduction in footpad thickness and parasite load compared to the untreated group. In addition, the average weight of the infected draining LNs was measured as a raw indicator of the parasite burden [19] and its decrease in OLEO-treated mice was in accordance with the respective reduced parasite burdens, demonstrating the reduced inflammatory effect at the site of infection. Recent scientific evidence showed suppressed footpad thickness in *L. major*- and *L. amazonensis*-infected mice using other plant-derived substances such as *Sambucus ebulus* aquatic extract and a coumarin isolated from leaves of *Calophyllum brasiliense*, respectively [29, 30], as well as the *Gossypium hirsutum* extract, which significantly decreases lesion size in *L. major*-infected mice [31].

The therapeutic potential of OLEO was further validated by histopathological data. In the murine model of CL, the successful control of parasites depends on local granulomatous inflammatory responses at the site of infection and the subsequent Th1-dominated systemic antigen-specific immune responses that control the progress of the infection [32]. Our analysis corroborated the clinical characteristics of footpad thickness and demonstrated OLEO's therapeutic efficacy. CD3+ central overexpression at the observed immature granulomas support the hypothesis of T cell-dependent responses detected in the lesions, which lead up to granuloma assembly. The observed increased monocyte influx, macrophage activation, and lysis at the necrotic granulomatous areas, due to persistent local particulate stimuli, *Leishmania* parasites in our case, all contribute to parasitic clearance [33]. Moreover, the observed mast cell degranulation enhances the therapeutic potential of OLEO since it has been reported that mast cells contribute to host defense against *Leishmania* spp. by actively taking up the parasite and by mounting effector responses for parasite clearance [34]. Additionally, it has been shown that dermal mast cells are required for the recruitment of macrophages during cutaneous granuloma formation [35]. Moreover, there is a report stating that *L. major*-infected mast cell-deficient $Kit^{(W)}/Kit^{(W\text{-}v)}$ mice developed larger skin lesions compared to wild-type mice [32].

Our data suggest the induction of a mixed Th1/Th2-type immune response in BALB/c mice, since both Th1-type (IL-12, INF-γ) and Th2-type (IL-4) cytokines are expressed, both Tbx21 and GATA-3 transcription factors genes are expressed, and a mixed humoral response is detected in the plasma. Nevertheless, the results reveal that OLEO is able to exert immunomodulation, as it favors the Th1-type immune response over Th2, which is crucial for the resolution of the infection in this mixed immunity background. The higher IgG2a/IgG1 ratio that was recorded after treatment with OLEO is related with Th1 prevalence in CL [36]. The segregation of IgG2a and IgG1 isotypes has been extensively used as a surrogate marker of protective Th1 and exacerbating

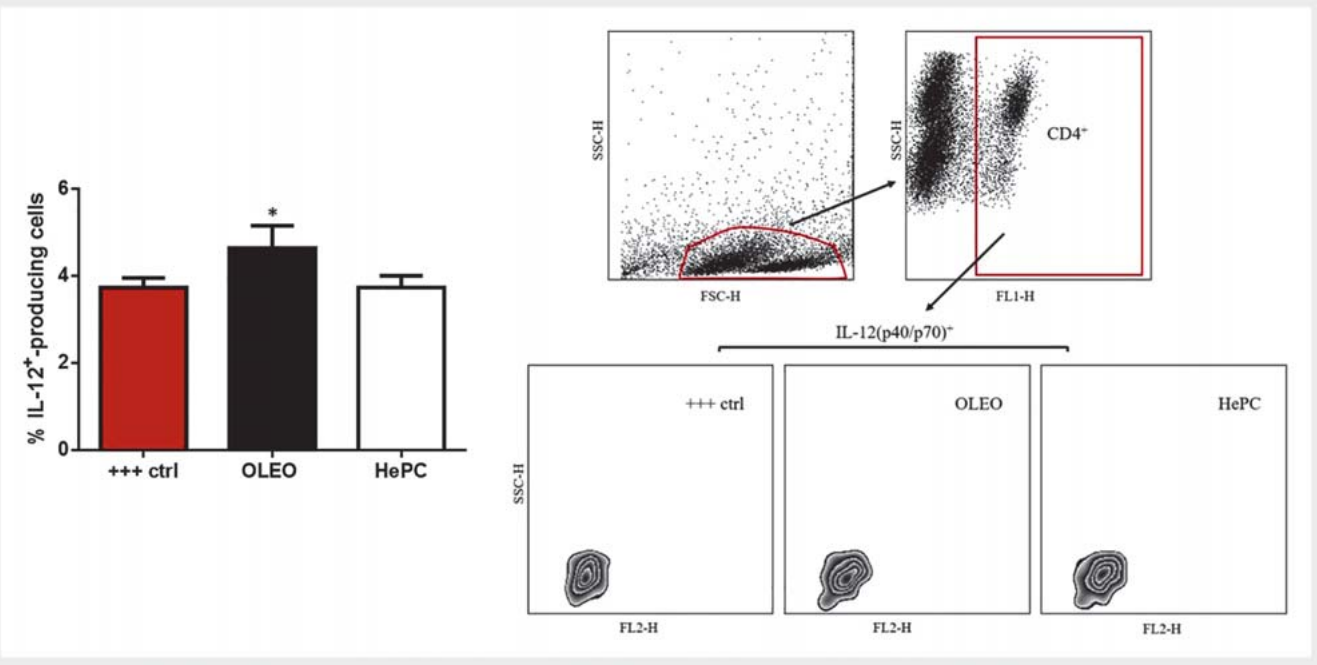

▶ **Fig. 7** Determination of IL-12$^+$-producing cells. The proportion of IL-12$^+$-producing cells in the spleen was assessed by flow cytometry 3 weeks after the termination of treatment. The results are expressed as mean values ± SD and are presented as a bar diagram and visualized as zebra plots. *Statistically significant differences compared to the control group (+++ctrl) of infected and untreated mice.

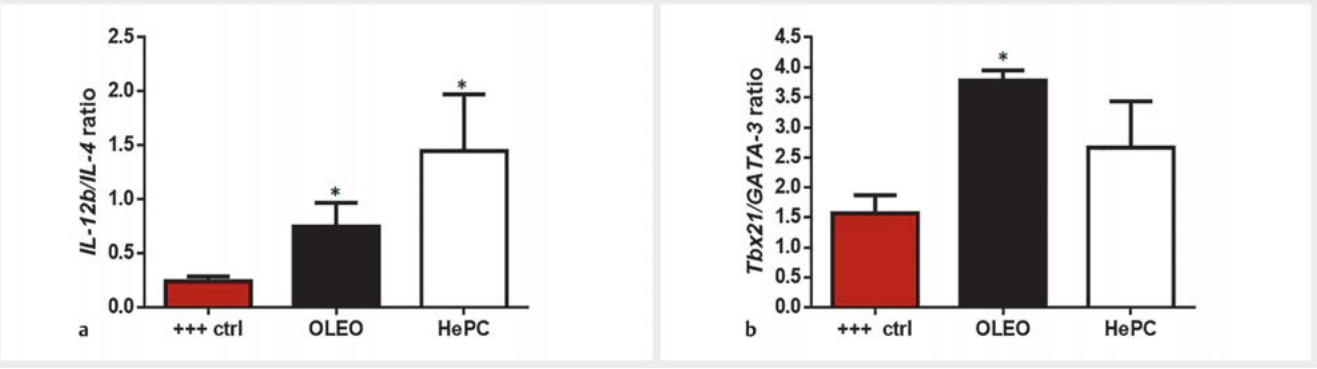

▶ **Fig. 8** Quantitative analysis of immune gene expression in splenocytes of BALB/c mice. The expression of cytokine genes *IL-12b* and *IL-4* (**a**) and transcription factor genes *Tbx21* and *GATA-3* (**b**) were determined with real-time PCR. All expression levels were computed via the *ΔΔCt* method. *Statistically significant differences compared to the control group (+++ctrl) of infected and untreated mice.

Th2 responses, respectively [37]. These findings are in accordance with our previous study where mice treated with the OLEO-enriched phenolic fraction also exhibited a higher IgG2a/IgG1 ratio [10]. The prevalence of Th1 immunity after treatment with OLEO was further validated by the induced IL-12 cytokine [38]. Furthermore, the elevated *Tbx21*/*GATA-3* gene expression ratios in OLEO-treated mice also confirms the orientation of T cell subpopulations towards the Th1-type response since it has been documented that the expression of these transcription factors is strongly associated with Th1 and Th2 polarization [20]. The immunomodulatory properties of OLEO have also been stated in other disease models. OLEO inhibited LPS-mediated upregulation of proinflammatory signaling molecules, including interleukin-1β, interleukin-6, macrophage inflammatory protein-1α, tumor necrosis factor-α, and granulocyte-macrophage colony-stimulating factor [39].

Overall, this study suggests that OLEO induces, *in vitro*, an efficient killing of *L. major* parasites and favors the Th1-type immune response in *L. major*-infected BALB/c mice. This research is the first comprehensive study conducted on the therapeutic effect of OLEO as an antiparasitic drug. OLEO is introduced as a novel candidate for alternative treatment of CL. Our findings suggest the potential use of OLEO in future immunotherapeutic strategies by challenging the status quo of today's chemotherapy and advocating new therapeutic protocols.

Material and Methods

Reagents and materials

The solvents *n*-hexane, *n*-heptane, ethyl acetate, ethanol, and water used for the extraction and isolation procedures were of analytical grade and purchased from CARLO ERBA Reagents. Acetonitrile, water, and formic acid used in UPLC-HRMS/MS analyses were of LC-MS grade and purchased from Fisher Scientific. $CDCl_3$ was used for ^{1}H-NMR experiments.

Selection of extra virgin olive oil

The EVOO used for the isolation of OLEO was freshly produced (January-February 2018) from olives of the "Koroneiki" variety harvested in Crete, Greece. The selected EVOO was found to be the richest in OLEO during a preliminary analysis of several freshly EVOOs produced from different varieties and in different areas of Greece. A specimen of the selected EVOO was stored in the herbarium of Division of Pharmacognosy and Natural Products Chemistry, Faculty of Pharmacy, NKUA (herbarium code: EVOO18-431_k-cr).

Isolation of pure oleocanthal from extra virgin olive oil

The isolation of pure OLEO from EVOO was achieved in a two-step separation process. The first step included the extraction of TPF from EVOO using a liquid-liquid extraction method. This procedure includes several "extraction-recovery" cycles using a 300-mL CPE column (FCPC Kromaton) and the biphasic system *n*-hexane/EVOO/ethanol/water at a ratio of 3/2/3/2 (v/v/v/v). In each "extraction-recovery" cycle, 2.5 L of EVOO containing an organic feed phase (mixing of 1 L of EVOO and 1.5 L of *n*-hexane) were pumped through 300 mL of extracting aqueous phase (ethanol/water at a ratio of 3/2) in ascending mode at flow rate 60 mL/min and a column rotation speed of 1000 rpm. The cycle was completed by switching the operating mode from ascending to descending and replacing the enriched TPF aqueous phase with a fresh one. The procedure was repeated 7 times and a total of 7 L of EVOO were treated. The collected TPF-containing aqueous phases were combined and evaporated to dryness, resulting in the recovery of 8.26 g of TPF.

The chromatographic isolation of OLEO included the initial fractionation of TPF by CPC and treatment of the enriched OLEO fractions by preparative HPLC. The CPC fractionation was run in a preparative (1000 mL) column (FCPC Kromaton) using a series of four biphasic systems [*n*-Hept/EtOAc/EtOH/water at ratios of 4/1/3/2, 3/2/3/2, 2/3/3/2, and 1/4/3/2 (v/v/v/v)] in step gradient elution-extrusion mode [22]. Eight grams of TPF were analyzed, leading to the recovery of 826 mg of OLEO-enriched fractions. The preparative HPLC purification was performed on a Supelco supelcosil TM LC-18 (Supelco Analytical) preparative column using mobile phase mixtures of water and acetonitrile in gradient elution [22]. An amount of 600 mg of the enriched fractions was analyzed and the peak of OLEO was collected manually based on UV chromatograms monitored at 275 nm, resulting in the recovery of 432 mg of pure OLEO. The purity (> 96 %) and structure confirmation of the isolated OLEO was achieved by UPLC-HRMS and NMR analysis (▶ **Fig. 9**).

Thin layer chromatography, ultra-performance liquid chromatography-HRMS, and NMR analysis

The CPC fractionation was monitored by TLC using silica gel 60 F254 aluminum plates (Merck). The chromatograms were developed using DCM or mixture of DCM and MeOH in different ratios. Spots were visualized on UV at 254 and 366 nm and were visible after spraying with sulfuric vanillin reagent [1 : 1 mixture of 5 % (v/v) H_2SO_4 in MeOH and 10 % (w/v) vanillin in MeOH] and heating the plates at 120 °C for 1 min.

The purity of the OLEO-enriched CPC fractions as well the isolated OLEO were checked by proton NMR experiments. The ^{1}H-NMR spectra were recorded on a Bruker Avance III 600 spectrometer (Bruker Biospin GmbH). The samples were diluted in 600 µL of $CDCl_3$ and analyzed at 25 °C using standard Bruker micro programs.

For purity control of the isolated OLEO, an H-Class Acquity UPLC system (Waters, Milford) coupled to an LTQ-Orbitrap XL hybrid mass spectrometer (Thermo Scientific) was also used. An amount of 100 µg of dry OLEO was dissolved in 1 mL of AcN : H_2O (4 : 1, v/v) and chromatographed on a Fortis C18 column (2.1 m × 100 µm i. d., 1.7 µm film thickness) while keeping the column temperature stable at 40 °C. The elution method used was as follows: solvent A – water acidified with 0.1 % formic acid, solvent B – acetonitrile, gradient mode: 0–3 min 5 % B, 3–21 min from 5 to 95 % B, 21–23 min 95 % B, 23–24 min from 95 to 5 % B, and 24 to 30 min 5 % B. The flow rate was 400 µL/min and the injection volume was 10 µL. Electrospray ionization was carried out in the negative ion mode using the following mass spectrometric parameters: capillary temperature 350 °C; sheath gas 40 units; aux gas 10 units; capillary voltage − 20 V; and tube lens − 80 V. Data were recorded in full scan from 115 to 1000 *m/z*. All experimental events were controlled using the software Xcalibur v.2.2 (Thermo Scientific).

Eukaryotic cell cultures

L. major (zymodeme LV39, strain MRHO/SU/59/P, isolation source: *Rhombomys opimus*, geographical isolation: USSR, ATCC No: 50 132) promastigotes were used and cultured in tissue flasks (Greiner) in complete RPMI-1640 medium (Biochrom). The *Leishmania* parasite strain was retained in a virulent state throughout a continuous passage in susceptible BALB/c mice. SLA was derived from 10^9 *L. major* stationary-phase promastigotes [12]. The immortalized macrophage cell line J774A.1 (ATCC No: TIB-67) was cultured in tissue flasks (Greiner).

Cell viability assay

The *in vitro* antileishmanial effect of OLEO was evaluated on stationary-phase *L. major* promastigotes and intracellular amastigotes using a resazurin-based cell viability assay [40]. Promastigotes were seeded in 96-well tissue culture plates at a concentration of 1×10^6 parasites/well (Sarstedt) and increasing concentrations of OLEO (2.5 to 150 µg/mL) were added in triplicate. HePC (Virbac) was used as a reference drug at the appropriate IC_{50} value, as previously described [11]. Plates were incubated at 26 °C for 60 h and then resazurin solution (20 µg/mL) (Sigma-Aldrich) was added. Plates were incubated until the observation of a fluores-

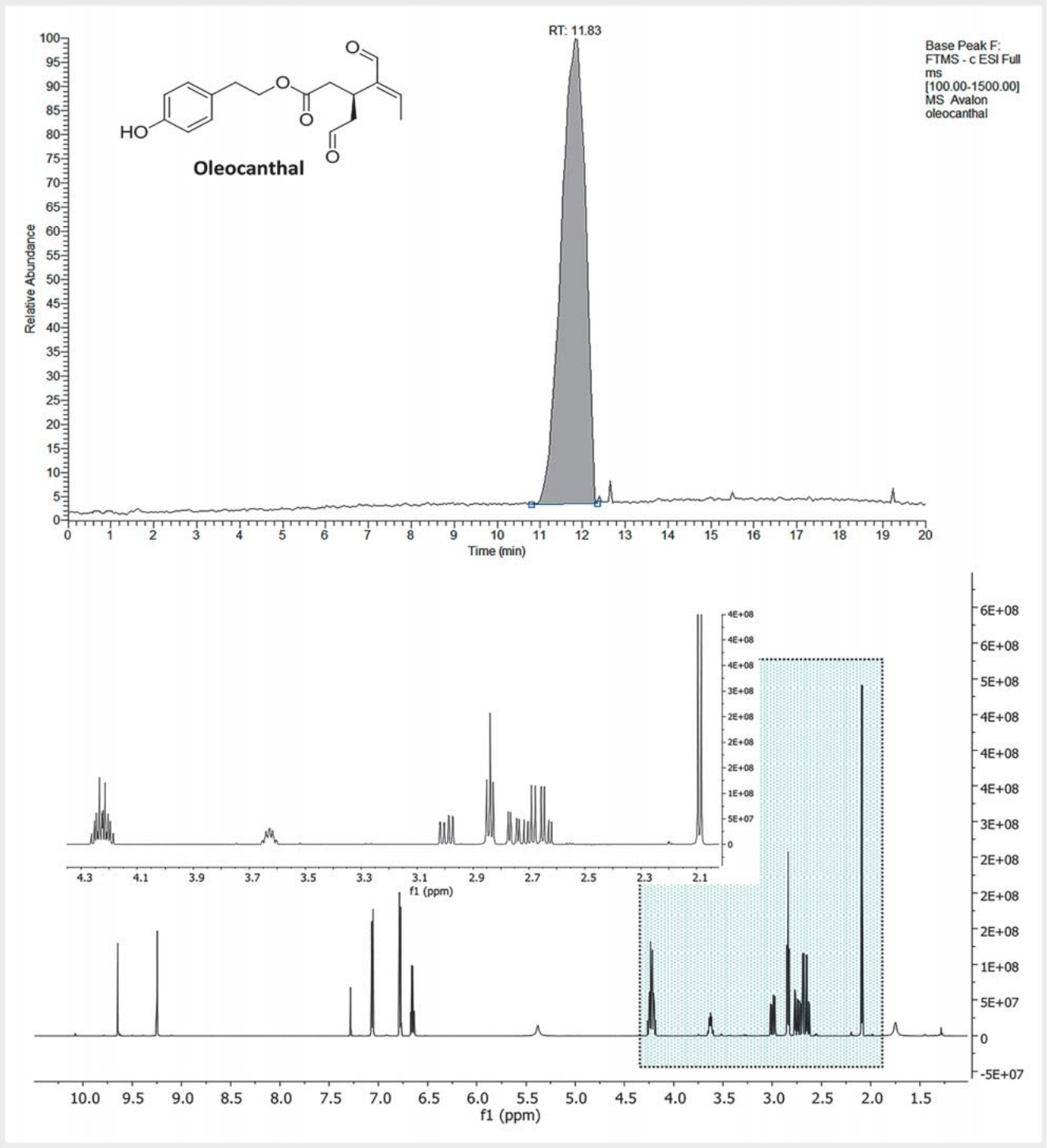

▶ **Fig. 9** Structure confirmation and purity evaluation of isolated OLEO using UPLC-HRMS (base peak chromatogram, left) and NMR spectroscopy (^{1}H-NMR spectrum, right).

cent red color in the negative control group (promastigotes cultured only in the presence of medium).

The evaluation of the anti-amastigote activity of OLEO was performed in *L. major* infected-J774A.1 macrophages [40]. Macrophages were added in 96-well plates at a concentration of 2.5×10^5 cells/well. The plates were incubated at 37 °C with 5% CO_2 for 18 h to achieve adhesion. Then, macrophages were infected with *L. major* stationary-phase promastigotes (15/1 ratio) for 48 h. Cells were then washed with RPMI-1640 medium to remove non-internalized parasites and OLEO was added at various increasing concentrations (2.5 to 200 µg/mL). *Leishmania*-infected macrophages cultured only in the presence of complete

RPMI-1640 medium were used as the negative control group. After 48 h of treatment at 37 °C and 5% CO_2, macrophages were lysed with 0.01% SDS, and Schneider's insect medium (Biosera) was added. The plates were further incubated at 26 °C for 72 h to allow transformation of viable amastigotes into promastigotes and proliferation. Resazurin solution (60 µg/mL) was added. Plates were incubated until the observation of a fluorescent red color in the negative control group. The ODs in both aforementioned procedures were determined using an absorbance microplate reader at 570 nm (reference filter at 630 nm).

The IC_{50} values were determined by point-to-point analysis with linear regression analysis and estimation of the coefficient of determination (R^2) and using the linear $y = ax + b$ equation (Microsoft Excel). This method assumes a linear relationship in the entire dose-response curve, which is rarely the case, as it typically has a sigmoidal shape. To employ this method for proper IC_{50} calculation, it usually has to be combined with the logarithmic transformation of one or both axes to ensure the proper conversion of the dose-response curve into the linear approximation [40].

Animals and ethics statements

Laboratory animals (mouse strain is BALB/cOlaHsd, supplied by Envigo) were maintained in specific pathogen-free conditions at the approved establishments of the Department of Animal Models for Biomedical Research in Hellenic Pasteur Institute (registered codes EL25BIOsup011, EL25BIObr012, EL25BIOexp013). The animals, age-matched (6–8 weeks old) female BALB/c mice (n = 18), were housed at room temperature (22 ± 2 °C), relative humidity of 40–70%, and a 12-h light/12-h dark cycle. All procedures complied to PD56/2013 and European Directive 2010/63/EU for welfare and ethical use of laboratory animals based on 3 + 1Rs and the guidelines of PREPARE and ARRIVEs, were approved by the Institutional Protocols Evaluation Committee, and were performed under the licensed protocol with registered code 6380/11–12–2017 (date of approval; December 11, 2017) by the Official Veterinary Authorities of Attica Prefecture.

Murine experimental model of cutaneous leishmaniasis and treatment schedule

Mice were infected s. c. with 1×10^6 *L. major* stationary-phase promastigotes at the left hind footpad. Ten days postinfection, mice were randomly assigned to three groups, OLEO-treated, HePC-treated, and untreated mice (control group). OLEO-treated mice received i. p. OLEO, 5 mg/kg b. w., every Monday, Wednesday, and Friday for 16 doses in total. HePC-treated mice received the reference drug HePC by oral gavage (per os) from Monday to Friday, at 15 mg/kg b. w., for 25 doses in total.

Monitoring of the infection progress

The thickness of the lesions at the injection site (left footpad) was monitored each week and recorded up to the end of the experiment. The increase of footpad thickness (mm) compared to the uninfected contralateral footpad was evaluated for all experimental groups using a dial gauge caliper (Mitutoyo).

Quantification of parasite burden by limiting dilution assay

The number of viable parasites in popliteal LNs was quantified by LDA [19]. Mice were sacrificed 3 weeks after the termination of treatment and popliteal LNs were dissected and weighed. Next, they were homogenized in 5 mL Schneider's insect medium supplemented with 20% FBS (ThermoFisher Scientific), and homogenates were diluted in 12 serial 2-fold dilutions and cultured in quadruplicate in sterile 96-well flat bottom microtiter plates (Sarstedt) at 26 °C for 10 days. The motile parasites were determined with an inverted microscope (OLYMPUS). The number of viable parasites/mg of tissue for each experimental group was calculated as mean and standard error of the highest dilution with live detectable parasites multiplied with the dilution factor whilst the total organ parasite burden was calculated using the weight of the respective organs [19].

Histopathological analysis

Three weeks after the termination of treatment, infected paws were fixed in paraformaldehyde solution 4% (overnight, RT), decalcified in EDTA 13% (pH 7.2) for 14 days, and embedded in paraffin. Serial paraffin sections (3 µm) were processed for histochemistry (H&E; Giemsa) and immunohistochemistry analysis. Antigen retrieval was achieved by heating sections in sodium citrate buffer (10 mM, pH 6) at 95 °C for 15 min, followed by blocking of endogenous peroxidase with 3% H_2O_2 in methanol and incubation with FBS (1/100 dilution) to block nonspecific immunoglobulin binding. Sections were incubated with monoclonal anti-CD20 and anti-CD3 (1/200; Agilent Dako) antibodies for 24 h at 4 °C, followed by biotinylated secondary antibodies and HRP-labeled avidin-biotin complex, and visualized using 3,3′-diaminobenzidine (Vector Laboratories). Slides were counterstained with Mayer's hematoxylin, dehydrated, cleared, and mounted. Isotype controls for nonspecific antibody binding were used. The tissue sections were analyzed by optical microscopy (Olympus BX-50 microscope) and images were captured with an Olympus DP71 microscope digital camera using Cell A imaging software (Soft Imaging System GmbH).

Detection of *Leishmania*-specific IgG antibodies

The *Leishmania*-specific IgG isotype profile was determined with ELISA tests using SLA obtained from *L. major* promastigotes. Three weeks after the termination of treatment, plasma from all experimental mice was analyzed for the presence of IgG1- and IgG2a-specific antibodies. Plates (Sarstedt) were coated with 5 µg/mL of SLA diluted in carbonate buffer (15 mM Na_2CO_3, 35 mM $NaHCO_3$), pH 9.6, and incubated overnight at 4 °C. Plates were blocked with 2% bovine serum albumin (AppliChem) and serial dilutions of plasma samples (1/20 to 1/40 960) were added. Then, plates were incubated with biotinylated anti-mouse IgG1 (500 ng/mL) or IgG2a (250 ng/mL) (AbDSerotec), and HRP streptavidin solution (1/5000, AbDSerotec) was added. Lastly, 3,3′,5,5′-tetramethylbenzidine substrate (ThermoFisher Scientific) was added, and absorbance was read at 450 nm. Results are expressed as antibody titer ± SD. Antibody titer was determined as the maximum dilution in which the sample's OD value was above the cutoff level (twice the mean value of blank wells).

Intracellular cytokine staining by flow cytometry

Splenocytes were aseptically collected 3 weeks after the termination of treatment. Then, 1×10^6 splenocytes were seeded in 24-well flat bottom plates (Sarstedt) and stimulated overnight with SLA (25 µg/mL) at 37 °C and 5% CO_2. Subsequently, cells were incubated with 2.5 µg/mL of brefeldin A (Fluka Chemie GmbH) for 4 h and then fixed with 2% w/v paraformaldehyde solution. The cells were permeabilized in permeabilization wash buffer (PBS + 3% FBS + 0.5% saponin) and stained with monoclonal antibodies for 30 min at 4 °C according to manufacturer's instructions. Staining was performed with the following anti-mouse monoclonal antibodies: FITC-CD4 (BD), PE-IL-4 (Biolegend), PE-IFN-γ (Biolegend), and PE-IL-12 (p40/p70) (BD). Control unstained samples were similarly processed for all the above cases. Then, 20 000 cells/sample were analyzed on FACSCalibur (BD) and acquired data were processed with FlowJo V.10.0.8 software (BD). Splenocytes were gated on forward light scatter and side light scatter to exclude debris and dead cells.

Gene expression analysis

Total mRNA was isolated from splenocytes obtained from all experimental mice 3 weeks after the termination of treatment using an RNeasy Mini kit (Qiagen). The mRNA concentrations and purities were determined with a NanoDrop2000 spectrophotometer (ThermoScientific) and cDNA synthesis was performed with a PrimeScripr RT-PCR Kit (Takara). Real-time PCR was performed using a SaCycler-96 Real-Time PCR System (Sacace Biotechnologies) with a KAPA SYBR FAST Universal Kit (KapaBiosystems). The specific primers for immune genes of interest [T-box transcription factor (*Tbx21*), trans-acting T cell-specific transcription factor (*GATA-3*), subunit 2 of interleukin 12 (*IL-12b*), interleukin-4 (*IL-4*), and glyceraldehyde dehydrogenase of the 3-phosphatase (*GAPDH*)] were designed by Qiagen (QuantiTect Primer Assays; Qiagen). All qPCR experiments were performed in three replicates, and non-template controls and reverse transcription controls were additionally performed. The PCR cycling conditions were as follows: 94 °C for 10 min, followed by 40 cycles at 94 °C for 10 s and 60 °C for 30 s. The expression level of GAPDH mRNA was used to normalize data of mRNA quantification, while the average of healthy controls was used as a calibrator. All expression levels were computed via the $\Delta\Delta Ct$ method [41].

Statistical analysis

The *in vitro* tests of anti-promastigote and anti-amastigote activities were performed in triplicate and the assays were repeated at least three times in independent experiments. All graphs were generated using GraphPad Prism 5 software (GraphPad Software, Inc.). Statistical analysis was performed with IBM SPSS Statistics v.24 software (IBM) using the two-sided Mann-Whitney test. Statistical differences were assumed significant at the 0.05 level of confidence.

Contributors' Statement

Conception and design of the work: K. Karampetsou, O. S. Koutsoni, F. Badounas, A. Angelis, A. L. Skaltsounis, M. Halabalaki, E. Dotsika; data collection: K. Karampetsou, O. S. Koutsoni, F. Badounas, A. Angelis, G. Gogou, A. L. Skaltsounis, M. Halabalaki, E. Dotsika; analysis and interpretation of the data: K. Karampetsou, O. S. Koutsoni, F. Badounas, A. Angelis, G. Gogou, A. L. Skaltsounis, M. Halabalaki, E.Dotsika; Statistical analysis: K. Karampetsou, O. S. Koutsoni, G. Gogou; drafting the manuscript: K. Karampetsou, O. S. Koutsoni, F. Badounas, A. Angelis, G. Gogou; critical revision of the manuscript: A. L. Skaltsounis, M. Halabalaki, E. Dotsika.

Acknowledgements

This work was supported by a PhD fellowship from the Hellenic Foundation for Research and Innovation (HFRI) (http://www.elidek.gr/) (GA. no.Ψ3B246ΨΖ2N-Σ3Γ). Also, part of this work was funded by the Operational Strategic Reference Framework (NSFR 2014–2020) (http://www.gsrt.gr) under Award Numbers MIS5002486 (KRIPIS) and MIS5028091 (EATRIS-GR).

Conflict of Interest

The authors declare that they have no conflict of interest.

References

[1] Mohammadbeigi A, Khazaei S, Heidari H, Asgarian A, Arsangjang S, Saghafipour A, Mohammadsalehi N, Ansari H. An investigation of the effects of environmental and ecologic factors on cutaneous leishmaniasis in the old world: a systematic review study. Rev Environ Health 2020; 36: 117–128

[2] Brindha J, Balamurali MM, Chanda K. An overview on the therapeutics of neglected infectious diseases-leishmaniasis and chagas diseases. Front Chem 2021; 9: 622286

[3] Johnston KL, Ford L, Taylor MJ. Overcoming the challenges of drug discovery for neglected tropical diseases: The A.WOL experience. J Biomol Screen 2014; 19: 335–343

[4] Ghodsian S, Taghipour N, Deravi N, Behniafar H, Lasjerdi Z. Recent researches in effective antileishmanial herbal compounds: Narrative review. Parasitol Res 2020; 119: 3929–3946

[5] Bulotta S, Celano M, Lepore SM, Montalcini T, Pujia A, Russo D. Beneficial effects of the olive oil phenolic components oleuropein and hydroxytyrosol: Focus on protection against cardiovascular and metabolic diseases. J Transl Med 2014; 12: 219

[6] Parkinson L, Cicerale S. The health benefiting mechanisms of virgin olive oil phenolic compounds. Molecules 2016; 21: 1734

[7] Tripoli E, Giammanco M, Tabacchi G, Di Majo D, Giammanco S, La Guardia M. The phenolic compounds of olive oil: Structure, biological activity and beneficial effects on human health. Nutr Res Rev 2005; 18: 98–112

[8] Pang KL, Chin KY. The biological activities of oleocanthal from a molecular perspective. Nutrients 2018; 10: 570

[9] Parkinson L, Keast R. Oleocanthal, a phenolic derived from virgin olive oil: A review of the beneficial effects on inflammatory disease. Int J Mol Sci 2014; 15: 12323–12334

[10] Karampetsou K, Koutsoni OS, Gogou G, Angelis A, Skaltsounis LA, Dotsika E. Total Phenolic Fraction (TPF) from extra virgin olive oil: Induction of apoptotic-like cell death in *Leishmania* spp. promastigotes and *in vivo* potential of therapeutic immunomodulation. PLoS Negl Trop Dis 2021; 15: e0008968

[11] Koutsoni OS, Karampetsou K, Kyriazis ID, Stathopoulos P, Aligiannis N, Halabalaki M, Skaltsounis LA, Dotsika E. Evaluation of total phenolic fraction derived from extra virgin olive oil for its antileishmanial activity. Phytomedicine 2018; 47: 143–150

[12] Kyriazis ID, Koutsoni OS, Aligiannis N, Karampetsou K, Skaltsounis AL, Dotsika E. The leishmanicidal activity of oleuropein is selectively regulated through inflammation-and oxidative stress-related genes. Parasit Vector 2016; 9: 441

[13] Sifaoui I, Lopez-Arencibia A, Martin-Navarro CM, Ticona JC, Reyes-Batlle M, Mejri M, Jimenezc AI, Lopez-Bazzocchi I, Valladares B, Lorenzo-Morales J, Abderabba M, Pinero JE. *In vitro* effects of triterpenic acids from olive leaf extracts on the mitochondrial membrane potential of promastigote stage of *Leishmania* spp. Phytomedicine 2014; 21: 1689–1694

[14] Sifaoui I, Lopez-Arencibia A, Martin-Navarro CM, Chammem N, Reyes-Batlle M, Mejri M, Lorenzo-Morales J, Abderabba M, Pinero JE. Activity of olive leaf extracts against the promastigote stage of *Leishmania* species and their correlation with the antioxidant activity. Exp Parasitol 2014; 141: 106–111

[15] Abuznait AH, Qosa H, Busnena BA, El Sayed KA, Kaddoumi A. Olive-oil-derived oleocanthal enhances beta-amyloid clearance as a potential neuroprotective mechanism against Alzheimer's disease: *In vitro* and *in vivo* studies. ACS Chem Neurosci 2013; 4: 973–982

[16] Akl MR, Ayoub NM, Mohyeldin MM, Busnena BA, Foudah AI, Liu YY, El Sayed KA. Olive phenolics as c-Met inhibitors: (−)-Oleocanthal attenuates cell proliferation, invasiveness, and tumor growth in breast cancer models. PLoS One 2014; 9: e97622

[17] Goren L, Zhang G, Kaushik S, Breslin PAS, Du YN, Foster DA. (−)-Oleocanthal and (−)-oleocanthal-rich olive oils induce lysosomal membrane permeabilization in cancer cells. PLoS One 2019; 14: e0216024

[18] Siddique AB, Ebrahim HY, Akl MR, Ayoub NM, Goda AA, Mohyeldin MM, Nagumalli SK, Hananeh WM, Liu YY, Meyer SA, El Sayed KA. (−)-Oleocanthal combined with lapatinib treatment synergized against HER-2 positive breast cancer *in vitro* and *in vivo*. Nutrients 2019; 11: 412

[19] Asad M, Bhattacharya P, Banerjee A, Ali N. Therapeutic and immunomodulatory activities of short-course treatment of murine visceral leishmaniasis with KALSOME10, a new liposomal amphotericin B. BMC Infect Dis 2015; 15: 188

[20] Kanhere A, Hertweck A, Bhatia U, Gokmen MR, Perucha E, Jackson I, Lord GM, Jenner RG. T-bet and GATA3 orchestrate Th1 and Th2 differentiation through lineage-specific targeting of distal regulatory elements. Nat Commun 2012; 3: 1268

[21] Angelis A, Hamzaoui M, Aligiannis N, Nikou T, Michailidis D, Gerolimatos P, Termentzi A, Hubert J, Halabalaki M, Renault JH, Skaltsounis AL. An integrated process for the recovery of high added-value compounds from olive oil using solid support free liquid-liquid extraction and chromatography techniques. J Chromatogr A 2017; 1491: 126–136

[22] Angelis A, Michailidis D, Antoniadi L, Stathopoulos P, Tsantila V, Nuzillard J, Renault J, Skaltsounis A. Pilot continuous centrifugal liquid-liquid extraction of extra virgin olive oil biophenols and gram-scale recovery of pure oleocanthal, oleacein, MFOA, MFLA and hydroxytyrosol. Sep Purif Technol 2021; 255: 117692

[23] Keyhani A, Sharifi I, Salarkia E, Khosravi A, Tavakoli Oliaee R, Babaei Z, Ghasemi Nejad Almani P, Hassanzadeh S, Kheirandish R, Mostafavi M, Hakimi Parizi M, Alahdin S, Sharifi F, Dabiri S, Shamsi Meymandi S, Khamesipour A, Jafarzadeh A, Bamorovat M. *In vitro* and *in vivo* therapeutic potentials of 6-gingerol in combination with amphotericin B for treatment of *Leishmania major* infection: Powerful synergistic and multifunctional effects. Int Immunopharmacol 2021; 101: 108274

[24] da Silva EF, Canto-Cavalheiro MM, Braz VR, Cysne-Finkelstein L, Leon LL, Echevarria A. Synthesis, and biological evaluation of new 1,3,4-thiadiazolium-2-phenylamine derivatives against *Leishmania amazonensis* promastigotes and amastigotes. Eur J Med Chem 2002; 37: 979–984

[25] Corware K, Harris D, Teo I, Rogers M, Naresh K, Muller I, Shaunak S. Accelerated healing of cutaneous leishmaniasis in non-healing BALB/c mice using water soluble amphotericin B-polymethacrylic acid. Biomaterials 2011; 32: 8029–8039

[26] Ayoub NM, Siddique AB, Ebrahim HY, Mohyeldin MM, El Sayed KA. The olive oil phenolic (−)-oleocanthal modulates estrogen receptor expression in luminal breast cancer *in vitro* and *in vivo* and synergizes with tamoxifen treatment. Eur J Pharmacol 2017; 810: 100–111

[27] Siddique AB, Ayoub NM, Tajmim A, Meyer SA, Hill RA, El Sayed KA. (−)-Oleocanthal prevents breast cancer locoregional recurrence after primary tumor surgical excision and neoadjuvant targeted therapy in orthotopic nude mouse models. Cancers (Basel) 2019; 11: 637

[28] Siddique AB, Ebrahim H, Mohyeldin M, Qusa M, Batarseh Y, Fayyad A, Tajmim A, Nazzal S, Kaddoumi A, El Sayed K. Novel liquid-liquid extraction and self-emulsion methods for simplified isolation of extra-virgin olive oil phenolics with emphasis on (−)-oleocanthal and its oral anti-breast cancer activity. PLoS One 2019; 14: e0214798

[29] Heidari-Kharaji M, Fallah-Omrani V, Badirzadeh A, Mohammadi-Ghalehbin B, Nilforoushzadeh MA, Masoori L, Montakhab-Yeganeh H, Zare M. *Sambucus ebulus* extract stimulates cellular responses in cutaneous leishmaniasis. Parasite Immunol 2019; 41: e12605

[30] Tiuman TS, Brenzan MA, Ueda-Nakamura T, Dias BP, Cortez DAG, Nakamura CV. Intramuscular and topical treatment of cutaneous leishmaniasis lesions in mice infected with *Leishmania amazonensis* using coumarin (−) mammea A/BB. Phytomedicine 2012; 19: 1196–1199

[31] Sharifi F, Sharififar F, Pournamdari M, Ansari M, Tavakoli Oliaee R, Bamorovat M, Khosravi A, Keyhani AR, Salarkia E, Mortazaeizdeh A, Dabiri S, Khamesipour A, Sharifi I. Leishmanicidal potentials of *Gossypium hirsutum* extract and its fractions on *Leishmania major* in a murine model: parasite burden, gene expression, and histopathological profile. J Med Microbiol 2021. doi:10.1099/jmm.0.001333

[32] Maurer M, Lopez Kostka S, Siebenhaar F, Moelle K, Metz M, Knop J, von Stebut E. Skin mast cells control T cell-dependent host defense in *Leishmania major* infections. FASEB J 2006; 20: 2460–2467

[33] Nylen S, Eidsmo L. Tissue damage and immunity in cutaneous leishmaniasis. Parasite Immunol 2012; 34: 551–561

[34] Naqvi N, Ahuja K, Selvapandiyan A, Dey R, Nakhasi H, Puri N. Role of mast cells in clearance of *Leishmania* through extracellular trap formation. Sci Rep 2017; 7: 13240

[35] von Stebut E, Metz M, Milon G, Knop J, Maurer M. Early macrophage influx to sites of cutaneous granuloma formation is dependent on MIP-1alpha/beta released from neutrophils recruited by mast cell-derived TNFalpha. Blood 2003; 101: 210–215

[36] Gamboa-Leon R, Vera-Ku M, Peraza-Sanchez SR, Ku-Chulim C, Horta-Baas A, Rosado-Vallado M. Antileishmanial activity of a mixture of *Tridax procumbens* and *Allium sativum* in mice. Parasite 2014; 21: 15

[37] Rostamian M, Sohrabi S, Kavosifard H, Niknam HM. Lower levels of IgG1 in comparison with IgG2a are associated with protective immunity against *Leishmania tropica* infection in BALB/c mice. J Microbiol Immunol Infect 2017; 50: 160–166

[38] Maspi N, Abdoli A, Ghaffarifar F. Pro- and anti-inflammatory cytokines in cutaneous leishmaniasis: A review. Pathog Glob Health 2016; 110: 247–260

[39] Scotece M, Gomez R, Conde J, Lopez V, Gomez-Reino JJ, Lago F, Smith AB 3rd, Gualillo O. Further evidence for the anti-inflammatory activity of oleocanthal: Inhibition of MIP-1alpha and IL-6 in J774 macrophages and in ATDC5 chondrocytes. Life Sci 2012; 91: 1229–1235

[40] Koutsoni OS, Karampetsou K, Dotsika E. *In vitro* screening of antileishmanial activity of natural product compounds: Determination of IC50, CC50 and SI values. Bio Protoc 2019; 9: e3410

[41] Livak KJ, Schmittgen TD. Analysis of relative gene expression data using real-time quantitative PCR and the 2(-Delta Delta C(T)) method. Methods 2001; 25: 402–408